Electronic Supplementary Material (ESI) for Dalton Transactions.
This journal is © The Royal Society of Chemistry 2016

Electronic Supplementary Information (ESI)

Oxygen Reduction Reaction Catalyzed by Nickel Complexes Based on Thiophosphorylated Calix[4]Resorcinols and Immobilized in Membrane Electrode Assembly of Fuel Cell

M.K. Kadirov,[a,b]* I.R. Knyazeva,[a] I.R. Nizameev,[a,c] R.A. Safiullin,[b] V.I. Matveeva,[a] K.V. Kholin,[a,b] V. V. Khrizanforova,[a] T.I. Ismaev,[b] A.R. Burilov,[a] Yu.H. Budnikova,[a] O.G. Sinyashin[a]

[a]A.E. Arbuzov Institute of Organic and Physical Chemistry, Kazan Scientific Center, Russian Academy of Sciences, 8, ul. Akad. Arbuzova, Kazan 420088, Russia.

[b]Kazan National Research Technological University, 68, ul. K. Marx, Kazan 420015, Russia.

[c]Kazan National Research Technical University, 10, ul. K. Marx, Kazan 420111, Russia.

E-mail: kamaka59@gmail.com.

List of supporting figures.

Figure S1. AFM image of 2x2 μm area of the complex ***2*** on a HOPG surface

Figure S2. AFM topography-image of 2x2 μm area of the complex ***2*** on a HOPG surface

Figure S3. AFM image of 5x5 μm area of the complex ***2*** on a HOPG surface

Figure S4. AFM topography-image of 5x5 μm area of the complex ***2*** on a HOPG surface

Figure S5. AFM image of 2x2 μm area of the complex ***1*** on a HOPG surface

Figure S6. AFM topography-image of 2x2 μm area of the complex ***1*** on a HOPG surface

Figure S7. AFM image of 5x5 μm area of the complex ***1*** on a HOPG surface

Figure S8. AFM topography-image of 5x5 μm area of the complex ***1*** on a HOPG surface

Figure S9. Polarization and power density curves for the H_2-O_2 fuel cell with the cathode of the organometallic catalyst ***1*** and Pt anode (entry 1 in Table 1)

Figure S10. Polarization and power density curves for the H_2-O_2 fuel cell with Pt cathode and the anode of the organometallic catalyst ***2*** (entry 4 in Table 1)

Figure S11. Polarization and power density curves for the H_2-O_2 fuel cell with both cathode and anode of Pt (entry 5 in Table 1)

Figure S12. The time dependence of the maximum power density after reaching optimum performance in a continuously operating FC with the MEA, the cathode side of which is the organometallic catalyst ***2*** and the anode - Pt / C catalyst.

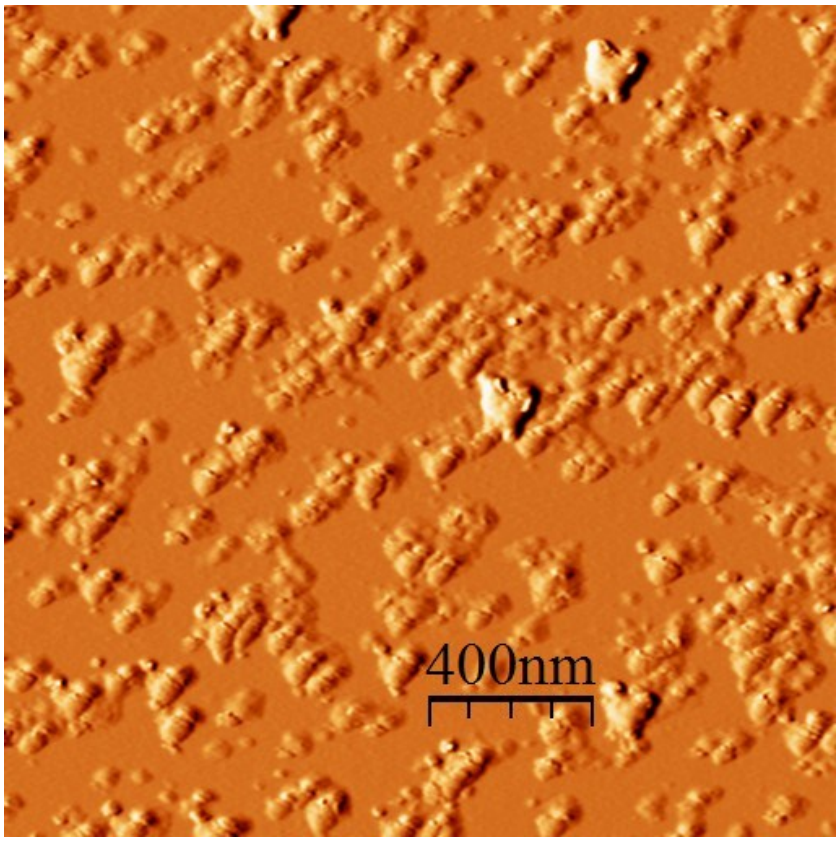

Figure S1. AFM image of 2x2 µm area of the complex ***2*** on a HOPG surface

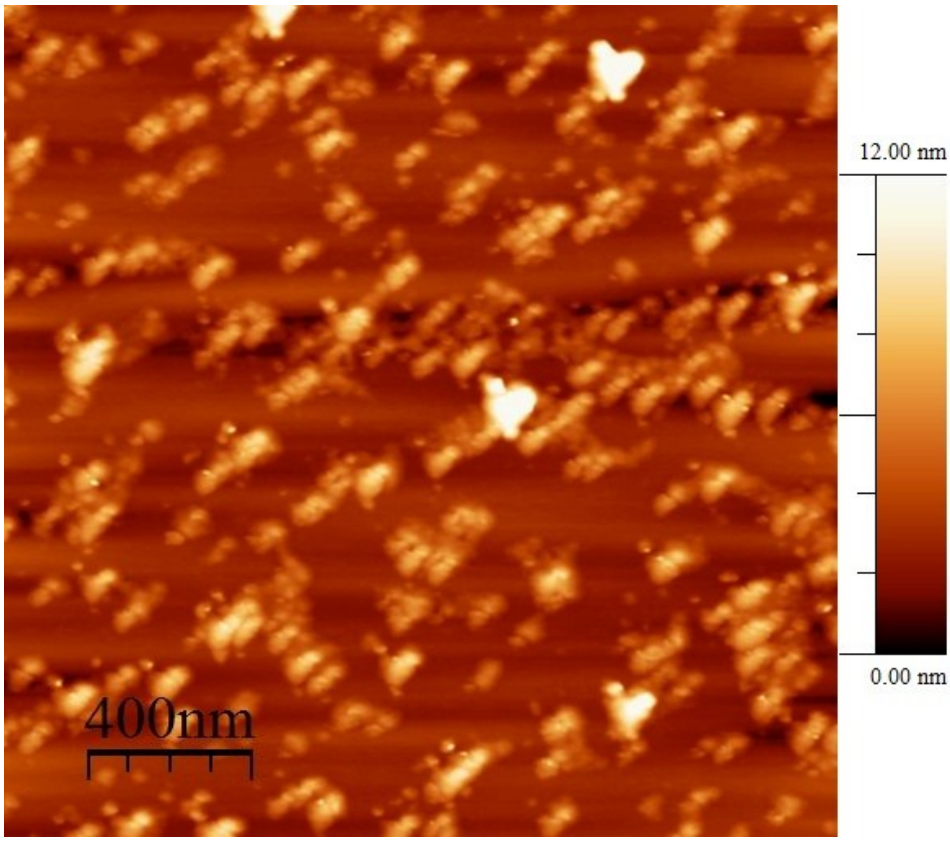

Figure S2. AFM topography-image of 2x2 µm area of the complex ***2*** on a HOPG surface

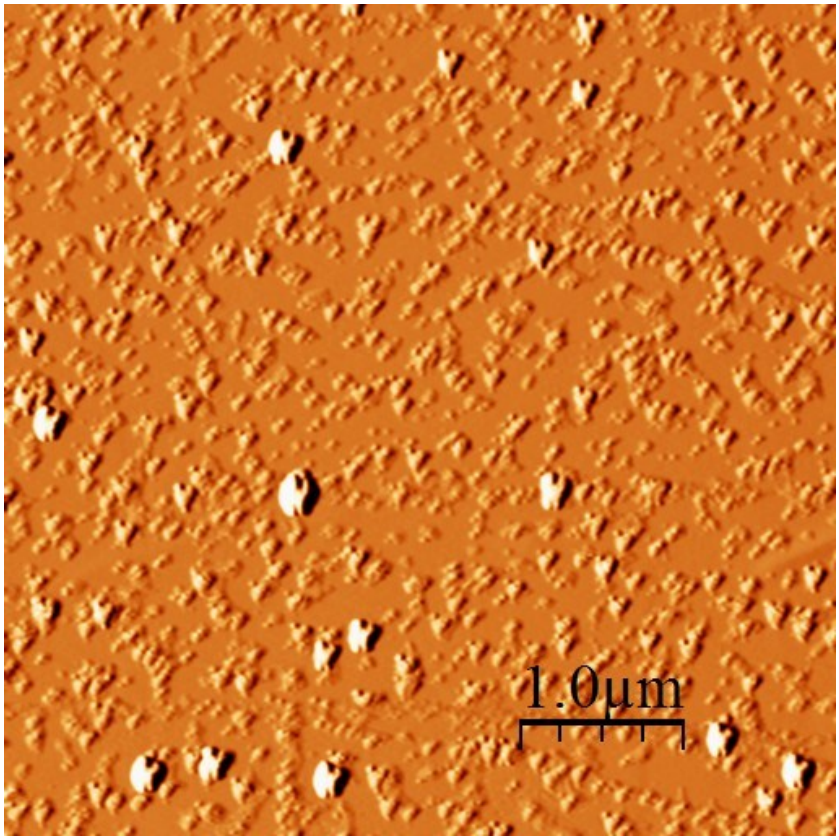

Figure S3. AFM image of 5x5 µm area of the complex ***2*** on a HOPG surface

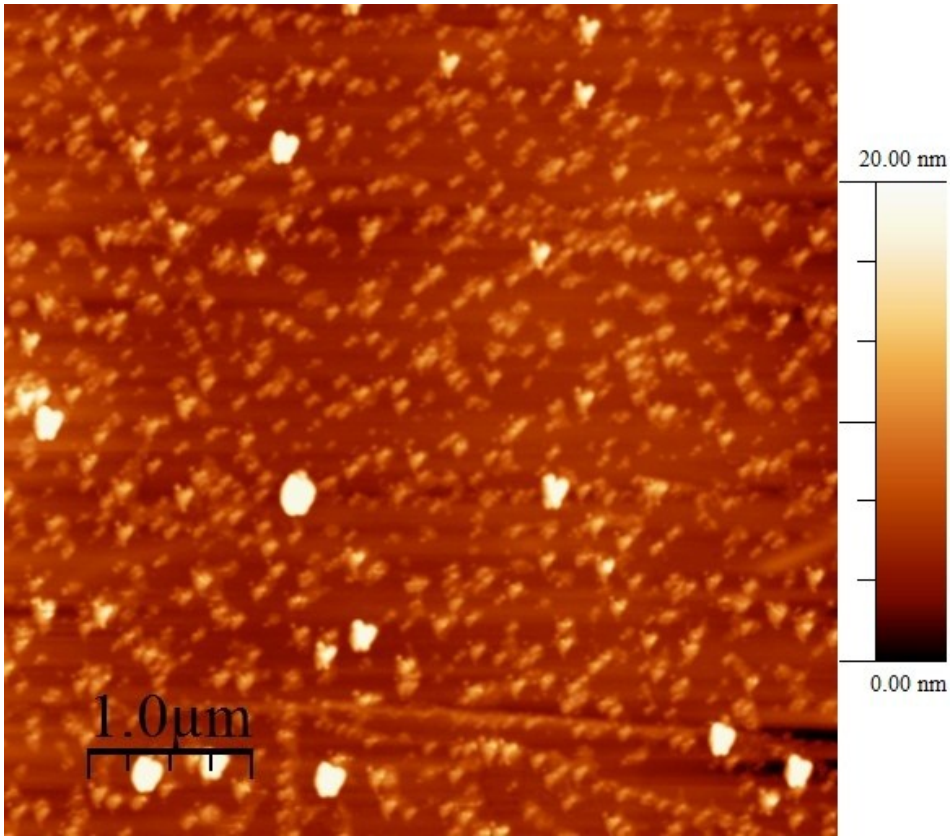

Figure S4. AFM topography-image of 5x5 µm area of the complex ***2*** on a HOPG surface

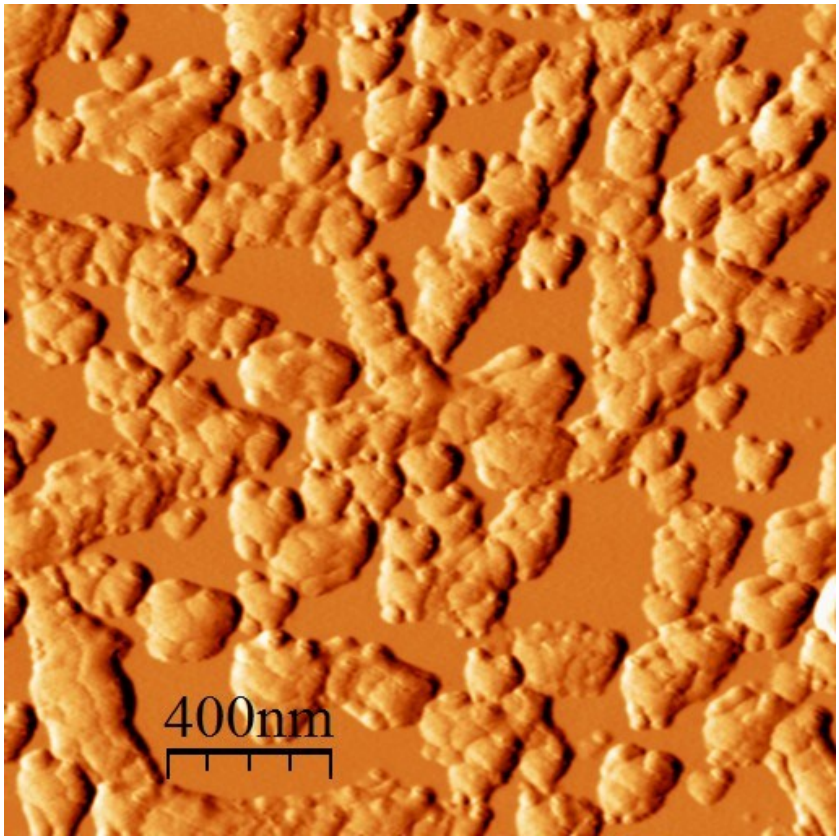

Figure S5. AFM image of 2x2 μm area of the complex ***1*** on a HOPG surface

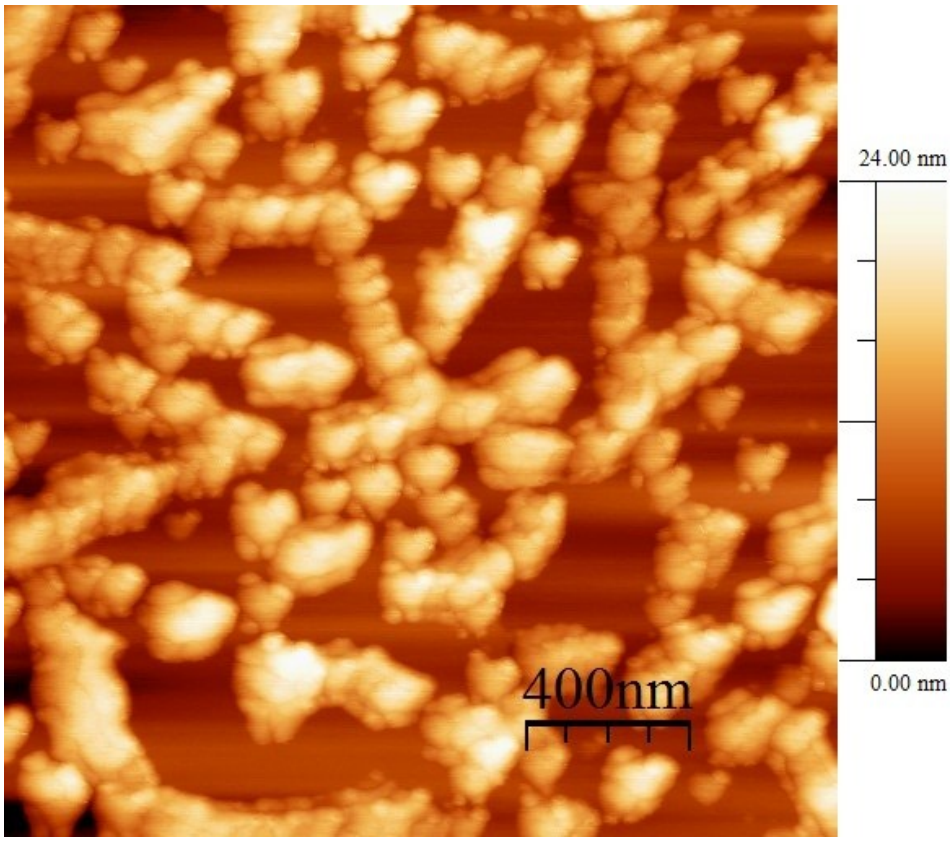

Figure S6. AFM topography-image of 2x2 μm area of the complex ***1*** on a HOPG surface

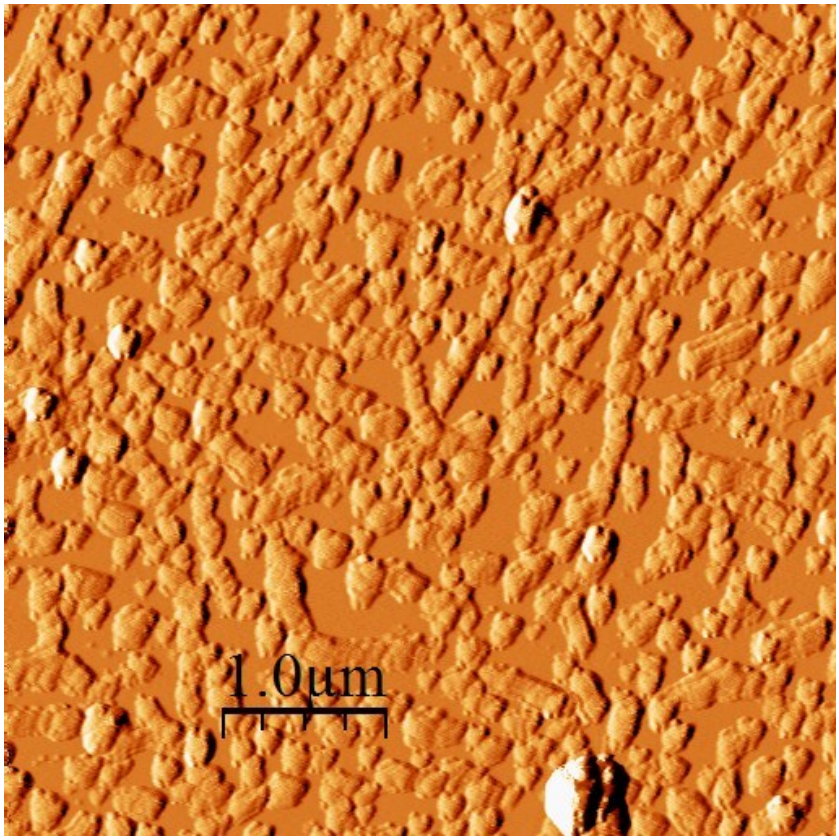

Figure S7. AFM image of 5x5 µm area of the complex ***1*** on a HOPG surface

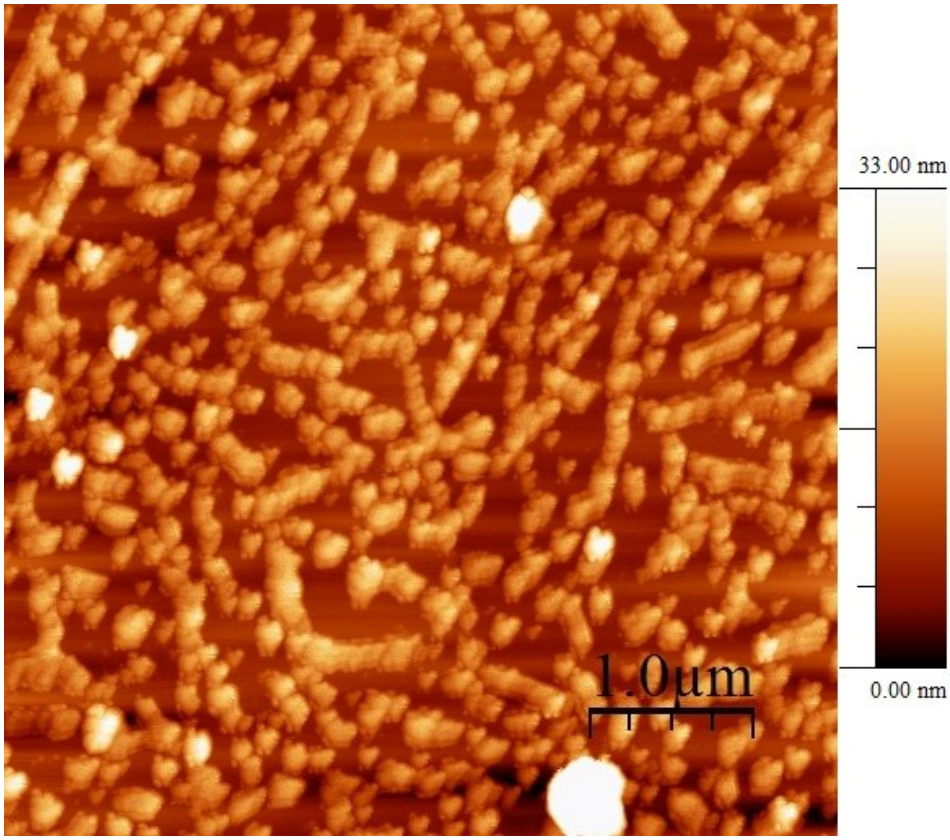

Figure S8. AFM topography-image of 5x5 µm area of the complex ***1*** on a HOPG surface

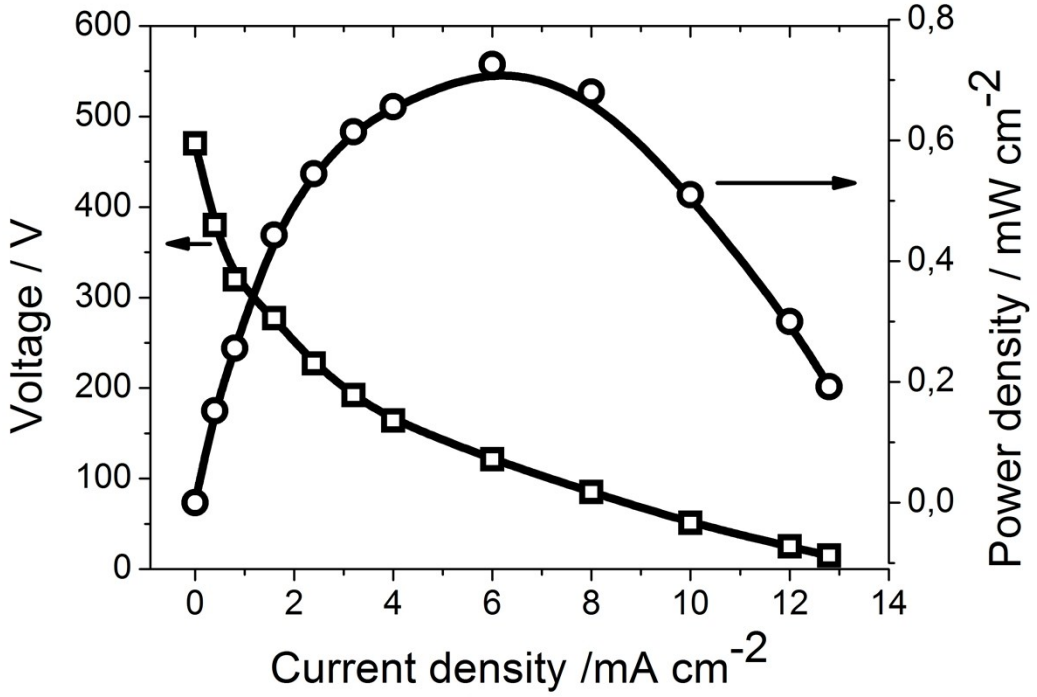

Figure S9. Polarization and power density curves for the H_2-O_2 fuel cell with the cathode of the organometallic catalyst ***1*** and Pt anode (entry 1 in Table 1)

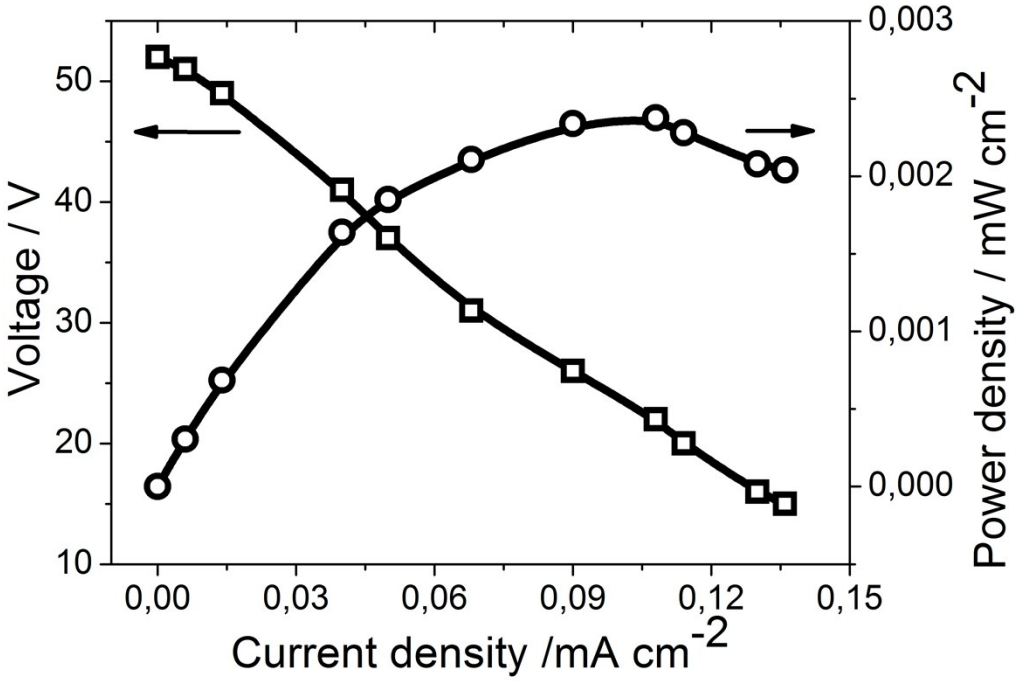

Figure S10. Polarization and power density curves for the H_2-O_2 fuel cell with Pt cathode and the anode of the organometallic catalyst ***2*** (entry 4 in Table 1)

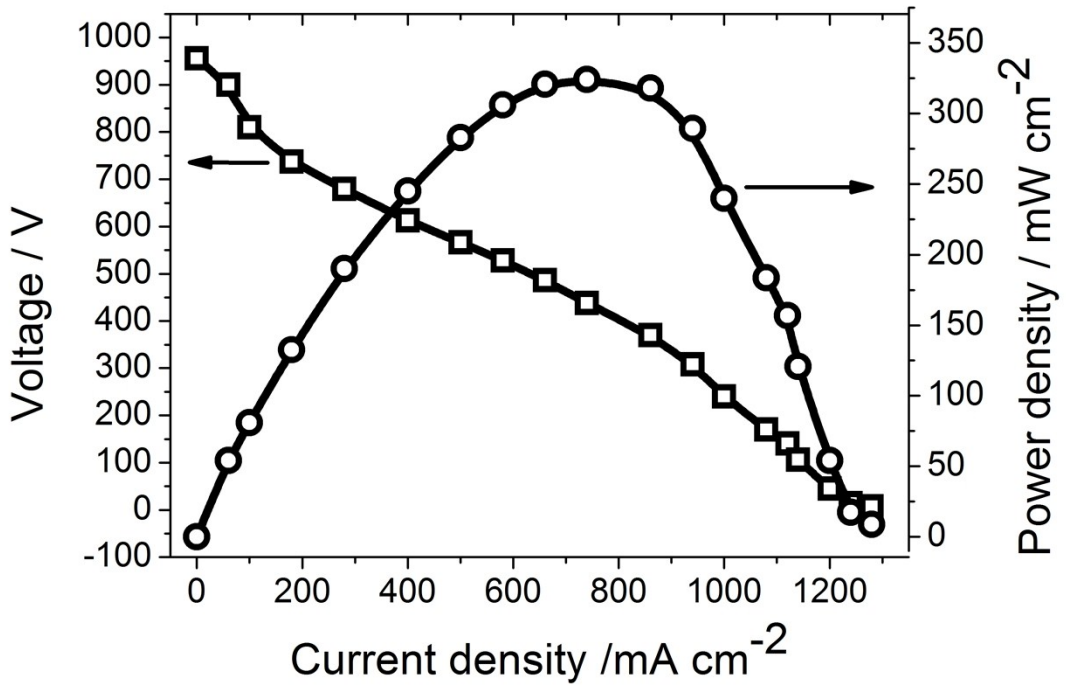

Figure S11. Polarization and power density curves for the H_2-O_2 fuel cell with both cathode and anode of Pt (entry 5 in Table 1)

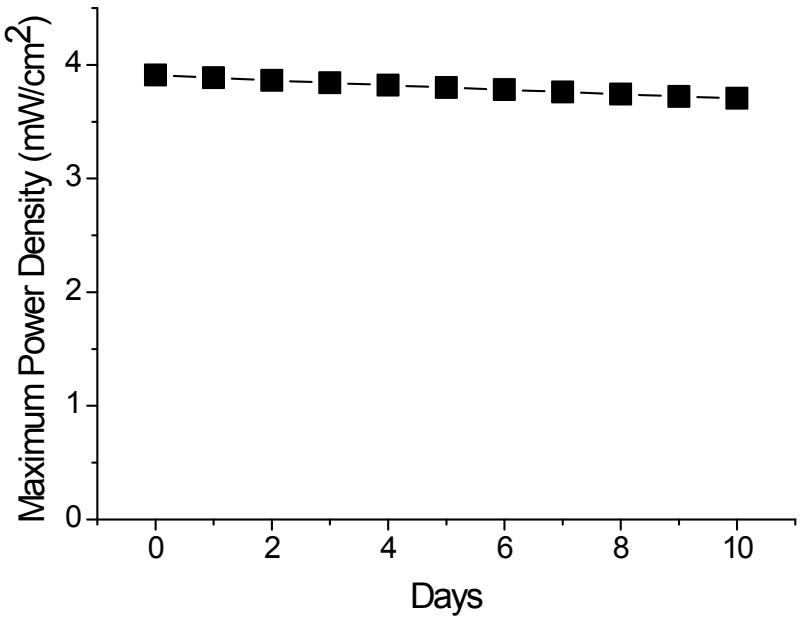

Figure S12. The time dependence of the maximum power density after reaching optimum performance in a continuously operating FC with the MEA, the cathode side of which is the organometallic catalyst ***2*** and the anode - Pt / C catalyst.

Nickel complexes with thiophosphorylatedcalixarenes have been prepared *in situ* by mixing 1 equiv. calixarene with 1 equiv. $Ni(BF_4)_2 \cdot 6H_2O$.

Ni^{2+}L (L in "chair" conformation): ^{1}H NMR (DMSO-d_6,) δ (ppm): 0.91 (s, 12H, CH_3), 1.14 (s, 12H, CH_3), 1.92 (s, 6H, CH_3), 2.11 (s, 6H, CH_3), 4.04 (m, 8H, OCH_2), 4.33 (m, 8H, OCH_2), 5.35 (s, 2H, CH_{ar}), 5.67 (s, 4H, CH), 6.15 (s, 2H, CH_{ar}), 6.66 (d, ^3J(H,H)=8.4 Hz, 8H, CH_{ar}), 6.83 (d, ^3J(H,H)=8.0 Hz, 8H, CH_{ar}), 7.44 (s, 4H, OH), 7.66 (s, 4H, OH). ^{31}P NMR (DMSO-d_6) δ (ppm): 54.4. MS MALDI-TOF: Calc. for $C_{76}H_{84}NiO_{20}P_4S_4$ *m/z* = 1626.27, Found: *m/z* = 1628.50.

Ni^{2+}L(L in "cone" conformation): ^{1}H NMR (DMSO-d_6,) δ (ppm): 0.91 (s, 12H, CH_3), 1,22 (s, 12H, CH_3), 1.91 (s, 12H, CH_3), 4.05 (m, 8H, OCH_2), 4.39 (m, 8H, OCH_2), 5.80 (s, 4H, CH), 6.09 (s, 4H, CH_{ar}), 6.74 (d, ^3J(H,H)=8.0 Hz, 8H, CH_{ar}), 6.95 (d, ^3J(H,H)=8.4 Hz, 8H, CH_{ar}), 7.56 мд (s, 8H, OH). ^{31}P NMR (DMSO-d_6) δ (ppm): 55.4. MS MALDI-TOF: Calc. for $C_{76}H_{84}NiO_{20}P_4S_4$ *m/z* = 1626.27, Found: *m/z* = 1628.30.